Ion beam emission in a low energy Plasma Focus device operating with methane

Article *in* Journal of Physics D Applied Physics · April 2005

DOI: 10.1088/0022-3727/38/8/011

5 authors, including:

Heman Bhuyan
Pontificia Universidad Católica de Chile
88 PUBLICATIONS **827** CITATIONS
SEE PROFILE

Mario Favre
Pontificia Universidad Católica de Chile
211 PUBLICATIONS **1,364** CITATIONS
SEE PROFILE

I. H. Mitchell
Merchiston Castle School
88 PUBLICATIONS **794** CITATIONS
SEE PROFILE

Edmund Wyndham
Pontificia Universidad Católica de Chile
166 PUBLICATIONS **979** CITATIONS
SEE PROFILE

INSTITUTE OF PHYSICS PUBLISHING JOURNAL OF PHYSICS D: APPLIED PHYSICS

J. Phys. D: Appl. Phys. **38** (2005) 1164–1169 doi:10.1088/0022-3727/38/8/011

Ion beam emission in a low energy plasma focus device operating with methane

H Bhuyan, H Chuaqui, M Favre[1], I Mitchell and E Wyndham

Pontificia Universidad Católica de Chile, Departamento de Física, Casilla 306, Santiago 22, Chile

E-mail: mfavre@fis.puc.cl

Received 30 December 2004, in final form 1 February 2005
Published 1 April 2005
Online at stacks.iop.org/JPhysD/38/1164

Abstract

An investigation of ion beam emission from a low energy plasma focus (PF) device operating with methane is reported. Graphite collectors, operating in the bias ion collector mode, are used to estimate the energy spectrum and ion flux along the PF axis, using the time-of-flight technique. The ion beam signals are time correlated with the emission of soft x-ray pulses from the pinched focus plasma. The correlation of ion beam intensity with filling gas pressure indicates that the beam emission is maximized at the optimum pressure for focus formation at peak current. Ion beam energy correlations for operation in methane indicate that the dominant charge states in carbon ions are C^{+4} and C^{+5}. The estimated maximum ion energy for H^+, C^{+4} and C^{+5} are in the range of 200–400 keV, 400–600 keV and 900–1100 keV, respectively, whereas their densities are maximum for the energy range 60–100 keV, 150–250 keV and 350–450 keV, respectively. These results suggest that the ion beams are emitted from a high density, high temperature, short lived focus plasma, at a time which appears to precede the emission of soft x-ray pulses. The properties of the carbon ion beams are discussed in the context of potential applications in materials science.

1. Introduction

In plasma focus (PF), a high density, high temperature, short duration plasma column is formed, following the radial compression phase that characterizes PF discharges [1]. In addition to x-ray and neutron pulses, the PF is a well-known source of energetic ion beams, of characteristic energy from hundreds of kiloelectronvolts to tens of megaelectronvolts [2, 3]. This characteristic energy range exceeds up to several hundred times the maximum energy to be expected from the capacitor bank voltage. Most of the earlier studies on ion beam emission in PF were carried out in deuterium medium, to investigate the correlation between neutron production and deuteron acceleration. Several properties of PF emitted deuteron beams have been measured, including their angular distributions and energy spectra [4–11]. A few investigations on ion beam emission in PF operating with other gases, such as hydrogen, helium, nitrogen and argon have also been reported [13–19]. Several theoretical and computational models on ion production and acceleration mechanisms have been developed for PF discharges [20–24]. Despite this theoretical effort, a complete explanation of the ion emission mechanism is still not available. Low energy PF operating in the few kilojoules range are characterized by a modest operational cost and allow easy modification. These particular features of PF devices, combined with the wide energy range and high characteristic flux of the emitted ion beams, together with the possibility of high frequency operation, have attracted the interest of several researchers, in view of the potential applications in different technological fields, such as surface properties modification, ion implantation, thin film deposition, semiconductor doping and ion-assisted coating [25–31]. Visualizing the importance of energetic carbon ions in the field of materials processing, we have performed an experimental analysis on axial ion emission from a low energy PF device operating in methane. The time-of-flight (TOF) technique [2] was used to measure the energy spectrum and the energy resolved ion flux, for the hydrogen and carbon ions identified in the beam composition. It is found that the main carbon ion beam components correspond to C^{+4} and C^{+5}. Based on the measured properties of the ion

[1] Author to whom any correspondence should be addressed.

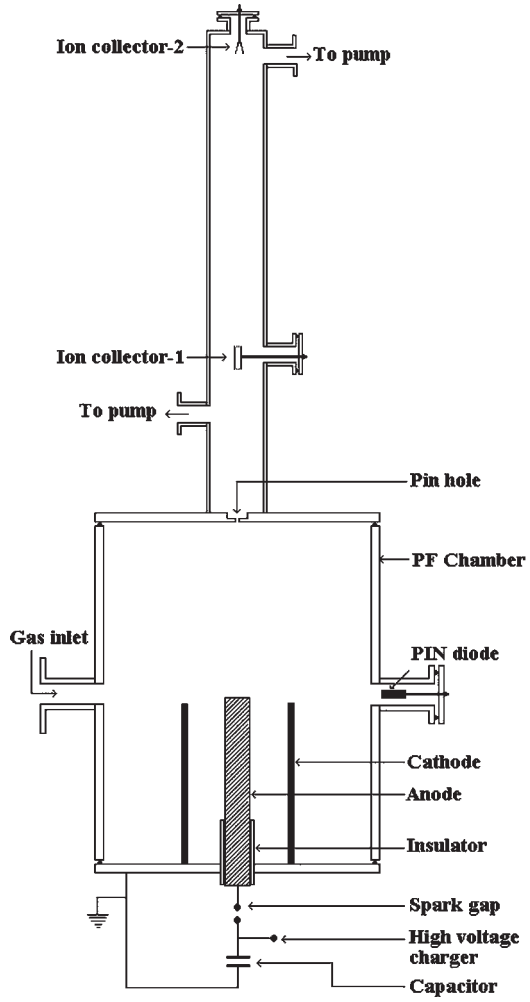

Figure 1. Experimental set-up.

beams, the plasma conditions at the time of ion emission are discussed in order to assess the validity of the current PF ion beam emission models.

2. Experimental apparatus

The present experiment was conducted in a low energy, 1.8 kJ, Mather [1] type PF device. A schematic diagram of the experimental arrangements along with the discharge circuit is shown in figure 1. The electrode assembly of the PF chamber consists of a hollow central anode of length 10 cm and outer diameter 2.4 cm encircled by six cathode rods of length 9.7 cm and diameter 0.8 cm uniformly spaced coaxially at a diameter of 6.3 cm. The electrode material is copper. The two electrodes are separated by a 3 cm long Pyrex glass insulator sleeve fixed around the bottom of the anode as shown in figure 1. The PF device is powered by a capacitor bank of 9 μF, at 30 kV maximum charging voltage. At 20 kV operating voltage the capacitor bank delivers a maximum current of 160 kA with 1.8 μs quarter period. The system inductance at the maximum current is around 146 nH. A resistive divider and a single groove Rogowski coil are used as voltage and current probes, respectively. Further details of the PF device were reported elsewhere [32]. The ion detection chamber, which acts as a drift tube, is separated from the PF chamber by a 15 mm diameter hole. In order to minimize the ion beam attenuation in the background gas medium the ion detection chamber is kept at a lower pressure than the main chamber, with the help of two additional pumps, as shown in figure 1. Two graphite collectors inside the drift tube were used to detect the axial ion beams emitted from the PF plasma: an open cylinder, 10 mm long, and of inner diameter 4 mm, located 50 cm away from the anode tip, and a cone, 15 mm in length with base diameter 4 mm, placed 110 cm away from the anode tip. Graphite is used as a collector material because of its reduced secondary electron emission coefficient. The collectors are negatively biased to a dc voltage of 200 V. Due to the negative biasing, the ion collectors also act as x-ray detectors (XRD). In this case, high energy photon illumination of the collectors results in a positive polarity signal. A BPX65 PIN diode masked with a 3 μm thick aluminium filter is placed at the side port of the PF chamber, to record the x-ray signal from the side-on plasma emission. In PF operation, intense soft x-ray pulses are mainly emitted at the time of maximum radial compression, when a hot and dense plasma column is formed. Because of the negative biasing, the ion probes also act as XRD. Thus, the x-ray emission recorded by the PIN diode and the x-ray signal in the ion probes can be used to establish a time correlation between plasma evolution and ion beam emission during the pinch formation process. The electrical signals from the voltage probe, current probe, PIN diode and ion probes are recorded on a four-channel, 500 MHz, 2 Gs s^{-1} sampling rate oscilloscope. Ion beam measurements were performed in methane and pure hydrogen, in the pressure ranges 0.2–0.45 Torr and 0.5–1.3 Torr, respectively.

3. Experimental results

Figure 2 shows oscillograms of voltage, current derivative, PIN diode and ion probe signals corresponding to operation at 0.35 Torr pressure. The singularities seen in the voltage and current derivative signals around 1.6 μs indicate strong PF action, which means that a tight, hot and dense plasma column has formed. The first peak in the ion probe signal is seen to coincide with both the x-ray pulse in the PIN diode and the singularities in the voltage and current derivative signals. After the x-ray peak, due to the photo-electron current, the ion probe signal exhibits a multi-peak structure, where at least three distinctive ion peaks, labelled 1–3, are identified, thus indicating either time delayed multi-beam emission, or a single multi-charged ion beam composition. The first possibility is ruled out, as TOF measurements using two ion probes indicate that the time delay between probes for the different beam components is consistent with simultaneous emission at a time which, within the time resolution, coincides with the emission of the x-ray pulse.This fact also allows single ion probe signals to be used for the ion energy spectrum measurements.

The time correlation between x-ray and ion beam emission indicates that in PF discharges ion acceleration takes place at some time around the maximum radial compression phase. Therefore, it is reasonable to assume that ion acceleration takes place in an existing plasma, with a multi-charged ion composition. Under these conditions, all ions are accelerated by the same electric field and the energy gained in the

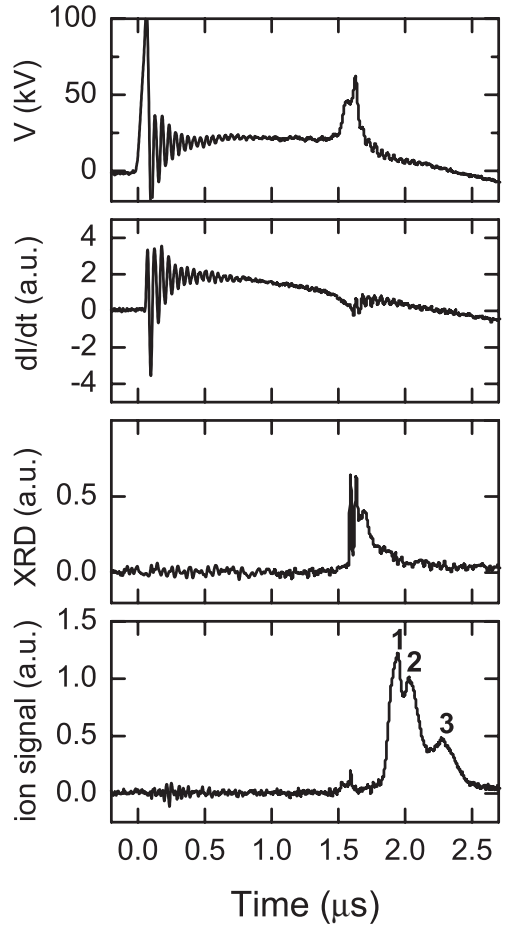

Figure 2. Characteristic signals at 0.35 Torr of methane. From top to bottom: voltage, time derivative of the discharge current, x-ray pin diode and ion probe signal. Labels 1, 2 and 3 identify three distinctive ion peaks.

acceleration process is proportional to the ion charge. This assumption, in the case of methane, allows us to use the following relation between the TOF of hydrogen ions, τ_{H}, and carbon ions of charge state n, $\tau_{n\mathrm{C}}$

$$\tau_{n\mathrm{C}} = \tau_{\mathrm{H}}\sqrt{\frac{M_{\mathrm{C}}}{nM_{\mathrm{H}}}}, \tag{1}$$

where M_{H} and M_{C} are the mass of the hydrogen and carbon ions, respectively.

A statistical procedure, based on over one hundred shots, was used to assign a characteristic TOF to the different peaks in the ion probe signals, prior to charge state identification. First, a peak deconvolution routine was applied to the ion probe signals, assuming a Gaussian shape for the different peaks. Second, characteristic TOFs where assigned to the onset and maximum value of the deconvolved peaks. Third, using equation (1) and assuming that the first ion peak in the ion probe signals corresponds to hydrogen, the charge state of the different subsequent carbon ion peaks was determined from the average values of the different measured TOFs.

Following identification of the charge state in the different beam components, the measured signal, together with the TOF information, can be used to determine the ion flux as a function of the ion energy for the observed charge states. A characteristic error in the ion energy can be estimated assuming that the uncertainty in the TOF is determined by the width of the initial x-ray pulse used as a time mark for the ion emission, which is of the order of 40 ns. Error bars in the ion energy spectra were calculated using the standard deviation over a number of shots. Figure 3 shows the ion flux as a function of energy for three different pressures, 0.31, 0.35 and 0.4 Torr. In each case, the error bar in the ion flux corresponds to the standard deviation over three shots. The error bars in the hydrogen spectrum have been cut off from the plots in order to highlight the features of the carbon ion spectra. The dominant carbon ion species are found to be C^{+4} and C^{+5}. The estimated errors in the energy spectrum at peak values are ±6 keV, ±9 keV and ±35 keV, for H^+, C^{+4} and C^{+5} ions, respectively. The presence of other ionization stages in the carbon ion spectrum was not observed within the energy resolution defined by the available

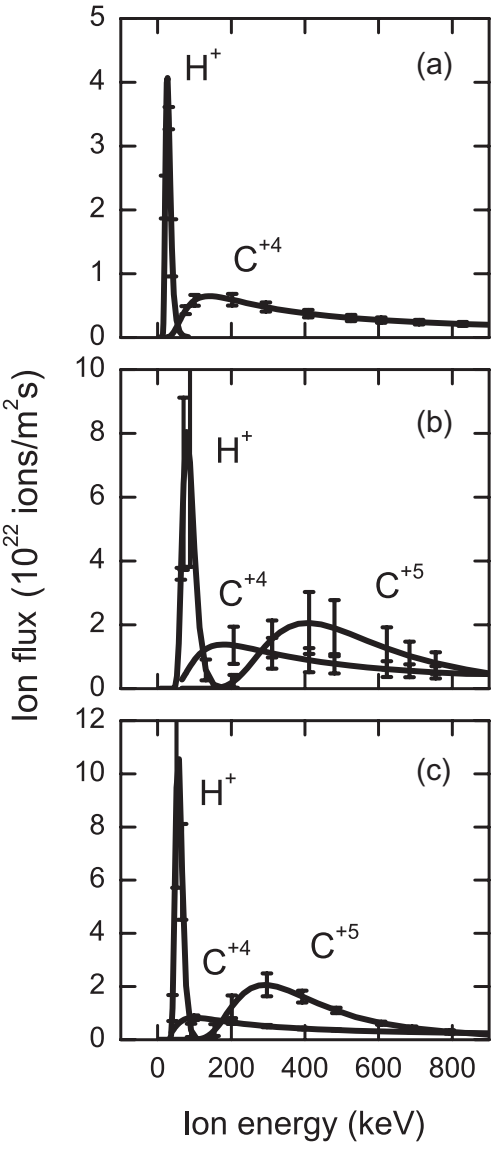

Figure 3. Energy spectrum for the different ion beam components at different pressures in methane. (*a*) 0.31 Torr, (*b*) 0.35 Torr and (*c*) 0.40 Torr.

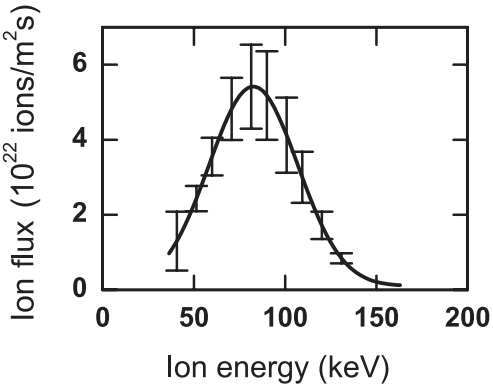

Figure 4. Energy spectrum for operation in pure hydrogen at 0.9 Torr.

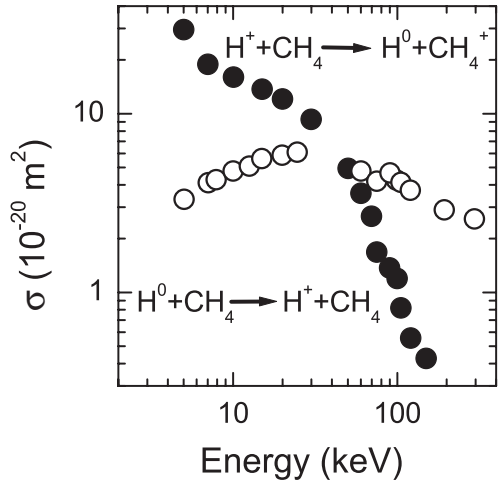

Figure 5. Cross sections for total charge exchange collisions between protons and neutral methane molecules (●) and ionizing collisions between neutral hydrogen atoms and neutral methane molecules (○) [33–36].

ion flight path. Similar results were obtained over the pressure range investigated. A series of shots with pure hydrogen as filling gas were conducted to compare the ion energy spectrum with that obtained with methane. Figure 4 shows the ion flux as a function of energy for a shot in pure hydrogen at 0.9 Torr. The error bars correspond to the standard deviation over five shots. The maximum ion energy for H^+, C^{+4} and C^{+5} are found to be in the range of 200–400 keV, 400–600 keV and 900–1100 keV, respectively, whereas their densities are maximum for the energy range 60–100 keV, 150–250 keV and 350–450 keV, respectively.

4. Discussion

Ion beam emission in PF discharges was originally investigated to explain the strong forward anisotropy observed in the neutron emission. In the case of small to medium energy PF devices, with capacitor bank energy up to a few tens of kilojoules, beam target processes involving axially directed deuteron beams were found to account for the observed anisotropy and neutron yield [2, 4, 5]. Measurements of the energy distribution function of deuterons were obtained using TOF detectors and Thomson analysers [2,3,6,8–12,14]. The energy spectrum of the deuterons was found to be in the 0.02–10 MeV range, for PF devices of characteristic bank energy in the 5–200 kJ range. Thomson analyser measurements also allowed the energy spectrum of heavier impurity ions to be determined together with the deuteron energy spectrum [5, 7, 14]. The characteristic energy of the different impurity ions was found, in general, to be proportional to the ion charge state, thus indicating a common acceleration mechanism for the deuterons and impurity ions. Measurements of the ion energy distribution in a 4.75 kJ PF operating with nitrogen, performed with a Thomson analyser, identified as the main ion species N^{+1}, N^{+2} and N^{+3}, with a characteristic energy in the range 0.17–4.0 MeV, and total (time integrated) average ion flux 8×10^{12} ions/stereorad [15]. The lower energy threshold was determined by the sensitivity of the detection system. Further measurements of the nitrogen ion energy spectrum in the same PF device using a TOF detector resulted in similar values of the average value of the ion flux [16]. In this case, the TOF signals did not allow the main ion charge states to be identified. TOF measurements have also been used to measure the ion spectrum of Argon ions in a 0.6 kJ PF, with no charge state identification [17]. The characteristic energy of the argon ions was found to be around 200 keV, with the energy spectrum extending up to 800 keV.

In our measurements, a path distance of 1.1 m allows the dominant carbon ion species to be identified. When the total number of carbon ions collected by the ion probe in a single shot is compared with the number of hydrogen ions, it is found that the hydrogen ions are around one tenth of the carbon ions, instead of a factor of four larger, as expected from the methane molecular composition. In order to explain this observation, it is important to note that the ion fluxes shown in figure 3 have not been corrected due to lateral spread and scattering or charge exchange collisions along the ion propagation path. The last two effects are particularly important for ion beam propagation inside the PF chamber, at the filling pressure, before the ions enter inside the drift tube. Figure 5 shows available data on the total cross sections for charge exchange collisions between protons and neutral methane molecules, and ionizing collisions between neutral hydrogen atoms and neutral methane molecules. It is seen that in the characteristic energy range of the hydrogen ions, 50–100 keV, the cross section for charge exchange collisions between protons and neutral methane molecules is higher than the cross section for ionizing collisions between neutral hydrogen atoms and methane molecules [33–36]. In both cases, the collisional mean free path is below one centimetre, for the pressure range 0.3–0.4 Torr. As the distance between the tip of the anode and the entrance to the drift tube is 15 cm, a substantial amount of hydrogen ion removal is expected from the axially propagating ions. A similar calculation for the propagation of the carbon ions cannot be performed, as no data on the charge exchange or ionization cross sections for collision between high charge state carbon ions and methane molecules in the range 100–600 keV has been found. At 40 keV, the charge exchange cross section for collisions between C^{+4} ions and CH_4 neutral molecules is 4.4×10^{-19} m^2 [37] and a single data point at 36 MeV gives a cross section value of 4.7×10^{-22} m^2, for the charge exchange collision between C^{+5} ions and CH_4 neutral molecules [38]. As the cross sections for

charge exchange collisions exhibit, in general, a monotonic logarithmic decrease towards higher energies, it is reasonable to assume that the cross sections for charge exchange collisions between high charge state carbon ions and CH_4 molecules in the 100–400 keV energy range are lower than the corresponding ones for hydrogen below 100 keV.

Despite the available experimental data, the exact mechanism for ion acceleration is still not clear. Basically, four different possibilities have been proposed to explain the ion beam formation. The first one is a re-distribution of current at the end of the radial compression phase, changing from an annular distribution to a centre peaked one, giving rise to intense, high gradient, axial electric fields [20], the second is an axial voltage increase due to a fast inductance change in the radial collapse phase [21], the third is ion runaway during the radial compression phase [22, 23] and the fourth is the formation of $m = 0$ MHD instabilities in the plasma column, which result in magnetic field energy being transferred to the kinetic energy of the ions [24]. The wide energy spectrum of the observed ion beams suggests a complex structure with different physical processes contributing to the formation of the beams. In our results, the carbon ion beam composition is seen to be dominated by C^{+4} and C^{+5} ions. In previous experiments performed in the same PF device, operating with a mixture of 80% hydrogen and 20% argon, measurements of the properties of hot-spots embedded in the pinched plasma column indicated a characteristic temperature in the range of 400–500 eV [39]. Figure 6 shows a calculation of the carbon ion composition of a carbon plasma made with the code FLY [40]. The calculation indicates that in the density range 10^{18}–10^{19} cm^{-3}, C^{+4} and C^{+5} ions are dominant only in a narrow temperature range around 50 eV. Although FLY calculations assume a given degree of thermodynamic equilibrium, which might not fully apply in this case due to the transient nature of the pinch formation process, the result is an indication that the ion acceleration does not take place at the maximum radial compression, when the higher temperature is achieved. This is in agreement with time correlated measurements of argon ion beams and x-ray emission in PF, which show that the ion emission starts before the x-ray emission, thus indicating that the energetic ions are emitted before the highest plasma temperature is achieved [17]. Although not totally conclusive, our results support the idea that ion acceleration in PF takes place at the early stages of pinch formation, where the developing of $m = 0$ MHD instabilities can provide a mechanism for energy transfer from the magnetic field to ions, as suggested by Vikhrev [24]. This is also supported by the fact that the characteristic energy of the hydrogen ions is similar when operating with pure hydrogen and methane, figures 3 and 4, as the available magnetic energy in the radial compression phase depends on the discharge current, which is determined by the electric and geometric parameters of the PF device. The observed energy spectrum, from a few tens of kiloelectronvolts up to over 1000 keV, is similar to that observed before in PF devices operating under similar conditions, with gas fillings other than deuterium [11, 15–18]; this also hints at a device parameter dependence of the ion beam properties.

Although several potential applications of PF ion beams in materials science have been reported [25–31], the use of PF generated carbon ions does not appear to have been explored.

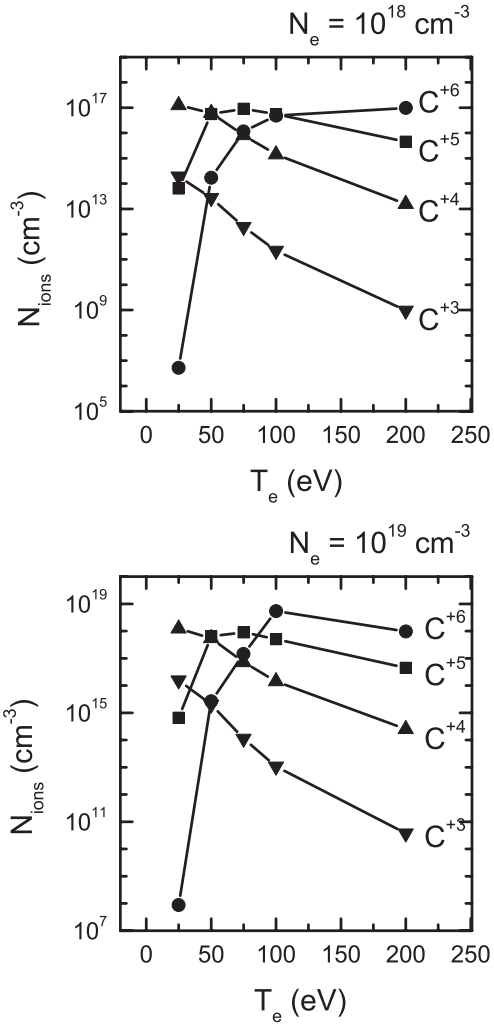

Figure 6. Calculated charge state composition of a carbon plasma, as a function of temperature and density.

Wide energy spectrum, short duration, carbon ion beams might find several potential applications in the field of carbon based nanotechnology. This is due to the high specific power density of the ion beams, which allows energy deposition on a given target to take place on a characteristic time scale much shorter than any time scale for heat conduction to the substrate. This is currently being explored and preliminary results will be reported elsewhere.

5. Conclusions

We have measured the basic properties, charge states, energy spectrum and flux, of ion beams generated in a low energy PF operating with methane. It has been found that for the operational conditions of the PF device the dominant charge states of the carbon ions are C^{+4} and C^{+5}, with maximum flux on-axis of the order of 2×10^{22} ions m^{-2} s, when operating with 0.35 Torr of methane. The dominant charge states of the carbon ions appear to be consistent with a model in which ion acceleration takes place before the high density, high temperature phase of the PF discharge. The measured ion beam parameters allow potential applications in materials science to

be explored, although some additional measurements, e.g. for beam divergence and radial distribution, need to be performed.

Acknowledgments

This work has been funded by FONDECYT grant 1030970 and ANDES Foundation grant C-13768. HB is funded by a postdoctoral grant from MECESUP and also acknowledges the Centre of Plasma Physics, Guwahati.

References

[1] Mather J W 1965 *Phys. Fluids* **8** 366
[2] Gerdin G, Stygar W and Venneri F J 1981 *J. Appl. Phys.* **52** 3269
[3] Sadowski M, Schmidt H and Herold H 1981 *Phys. Lett.* A **83** 435
[4] Gullickson R L and Sahlin H L 1978 *J. Appl. Phys.* **49** 1099
[5] Bertalot L, Herold H, Jäger U, Mozer A, Oppenländer T, Sadowski M and Schmidt H 1980 *Phys. Lett.* A **79** 389
[6] Yamada Y, Kitagawa Y, Yokoyama M and Yamanaka C 1981 *Phys. Lett.* A **83** 9
[7] Sadowski M, Źebrowski J, Rydygier E, Herold H, Jäger U and Schmidt H 1985 *Phys. Lett.* A **113** 25
[8] Sadowski M, Źebrowski J, Rydygier and Kuciński J 1988 *Plasma Phys. Control. Fusion* **30** 763
[9] Bostick W H, Kilic H, Nardi V and Powell C W 1993 *Nucl. Fusion* **33** 413
[10] Kelly H and Márquez A 1996 *Plasma Phys. Control. Fusion* **38** 1931
[11] Sadowski M, Sadowska E S, Baranowski J, Źebrowski J, Kelly H, Lepone A, Márquez A, Milanese M, Moroso R and Pouzo J 2000 *Nukleonika* **45** 179
[12] Hirano K, Yamamoto T, Okabe Y and Shimoda K 1987 *Rev. Sci. Instrum.* **58** 20
[13] Rhee M J 1980 *Appl. Phys. Lett.* **37** 906
[14] Mozer A, Sadowski M, Herold H and Schmidt H 1982 *J. Appl. Phys.* **53** 2959
[15] Kelly H, Lepone A and Márquez A 1997 *IEEE Trans. Plasma Sci.* **25** 455
[16] Kelly H, Lepone A, Márquez A, Sadowski M J, Baranowski J and Skladnik-Sadowska E 1998 *IEEE Trans. Plasma Sci.* **26** 113
[17] Heo H and Park D K 2002 *Phys. Scr.* **65** 350
[18] Takao K, Honda T, Kitamura I and Masugata K 2003 *Plasma Sources Sci. Technol.* **12** 407
[19] Bhuyan H, Mohanty S R, Borthakur T K and Rawat R S 2001 *Indian J. Pure Appl. Phys.* **39** 698
[20] Bernstein M J 1970 *Phys. Fluids* **13** 2858
[21] Browne P F 1988 *J. Phys. D: Appl. Phys.* **21** 596
[22] Deutsch R and Kies W 1988 *Plasma Phys. Control. Fusion* **30** 263
[23] Deutsch R and Kies W 1988 *Plasma Phys. Control. Fusion* **30** 921
[24] Vikhrev V V 2004 *Proc. 15th Int. Conf. on High-Power Particle Beams (Saint Petersburg, Russia)* submitted
[25] Gribkov V A *et al* 2003 *J. Phys. D: Appl. Phys.* **36** 1817
[26] Feugeas J, Lionch E C, de González C O and Galambos G 1988 *J. Appl. Phys.* **64** 2648
[27] Sagar R and Srivastava M P 1993 *Phys. Lett.* A **183** 209
[28] Kelly H, Lepone A, Marquez A, Lamas D and Oviedo C 1996 *Plasma Sources Sci. Technol.* **5** 1
[29] Sánchez G and Feugeas J 1997 *J. Phys. D: Appl. Phys.* **30** 927
[30] Nayak B B, Acharya B S, Mohanty S R, Borthakur T K and Bhuyan H 2001 *Surf. Coat. Technol.* **145** 8
[31] Rawat R S, Lee P, White T, Ying L and Lee S 2001 *Surf. Coat. Technol.* **138** 159
[32] Favre M, Silva P, Choi P, Chuaqui H, Dumitrescu C and Wyndham E 1998 *IEEE Trans. Plasma Sci.* **26** 1154
[33] Rudd M E, DuBois R D, Toburen L H, Ratcliffe C A and Goffe T V 1983 *Phys. Rev.* A **28** 3244
[34] Sanders 2003 *J. Phys. B: At. Mol. Phys.* **36** 3835
[35] McNeal R J 1970 *J. Chem. Phys.* **53** 4308
[36] Toburen L H 1968 *Phys. Rev.* **171** 114
[37] Soejima K 1993 *Org. Mas. Sp.* **28** 344
[38] Woods C J 1984 *J. Phys. B: At. Mol. Phys.* **17** 867
[39] Silva P and Favre M 2002 *J. Phys. D: Appl. Phys.* **53** 2543
[40] FLY, Atomic Kinetics Code, Cascade Applied Sciences, Boulder CO 80306, USA